Supplementary Information

Two-dimensional GeTe nanosheets for psoriasis through modulation of macrophage activation and psoriatic inflammation

Jieun Han,[a,b] Ju-Won Kim,[a,b] In Kang,[a] Sun-Mi Lee*[a] and Yong-Beom Park*[a,b,c]

[a] Division of Rheumatology, Department of Internal Medicine, Yonsei University College of Medicine, Seoul, 03722, Republic of Korea

[b] Brain Korea 21 PLUS Project for Medical Science, Yonsei University College of Medicine, Seoul, 03722, Republic of Korea

[c] Institute for Immunology and Immunological Diseases, Yonsei University College of Medicine, Seoul, 03722, Republic of Korea

* Co-corresponding authors: sunmilee@yuhs.ac, yongbpark@yuhs.ac

Section 1. Experimental Section

Enzyme-linked immunosorbent assay (ELISA)

The levels of IL-1β and IL-6 in the supernatant samples of RAW 264.7 cells were analyzed using ELISA kits according to the manufacturers' instructions. IL-1β and IL-6 levels were measured using the BD OptEIA™ Mouse IL-1β ELISA Set and BD OptEIA™ Mouse IL-6 ELISA Set (BD Biosciences, Franklin Lakes, NJ, USA), respectively.

Immunofluorescence staining of skin tissues

Immunofluorescence (IF) staining was performed to evaluate the expression of F4/80, CD4, and filaggrin in skin lesions. Dorsal skin samples were collected from mice and fixed with 10% formalin for 72 h. The tissues were subsequently dehydrated, embedded in paraffin, and sectioned into 4-μm thick slices. Paraffin sections were deparaffinized and rehydrated through a graded ethanol series. Antigen retrieval was conducted using 1M sodium citrate buffer (pH 6.0; Biosolution, Seoul, Republic of Korea). Endogenous peroxidase activity was quenched by incubation with 3% hydrogen peroxidase for 10 min, followed by washing with Tris-buffered saline (TBS) buffer. The slides were incubated overnight at 4°C with primary antibodies against F4/80 (Invitrogen, Carlsbad, CA, USA), CD4 (Santa Cruz Biotechnology, Dallas, TX, USA), and filaggrin (BioLegend, San Diego, CA, USA). After washing with TBS buffer, the samples were further stained with secondary antibodies (Invitrogen) for 1 h in room temperature. Finally, nuclei were counterstained using antifade mounting medium containing DAPI (Vector Laboratories, Newark, CA, USA). IF images were obtained with a Zeiss LSM 780 confocal microscope (Carl Zeiss MicroImaging GmbH, Oberkochen, Germany) and analyzed with Zen 3.1 software and ImageJ.

Section 2. Figures

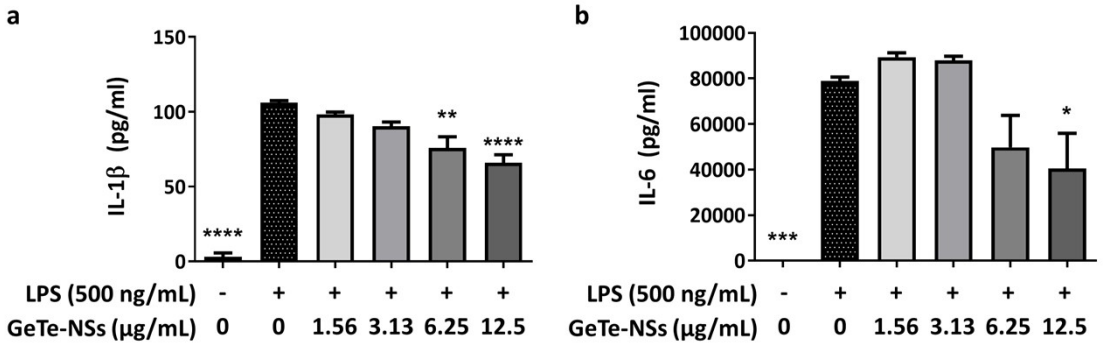

Fig. S1. Regulation of GeTe-NSs on LPS-induced IL-1β and IL-6 release in RAW 264.7 cells. RAW 264.7 cells were treated simultaneously with LPS (500 ng/mL) and the indicated concentrations of GeTe-NSs. After 24 h incubation, the cytokine levels of (a) IL-1β and (b) IL-6 in the supernatants were measured by ELISA kits. All data are presented as the mean ± SEM for three independent experiments. Statistical significance was determined by one-way ANOVA in comparison with the LPS-stimulated RAW 264.7 samples. *$p < 0.05$, **$p < 0.01$, ***$p < 0.001$, ****$p < 0.0001$.

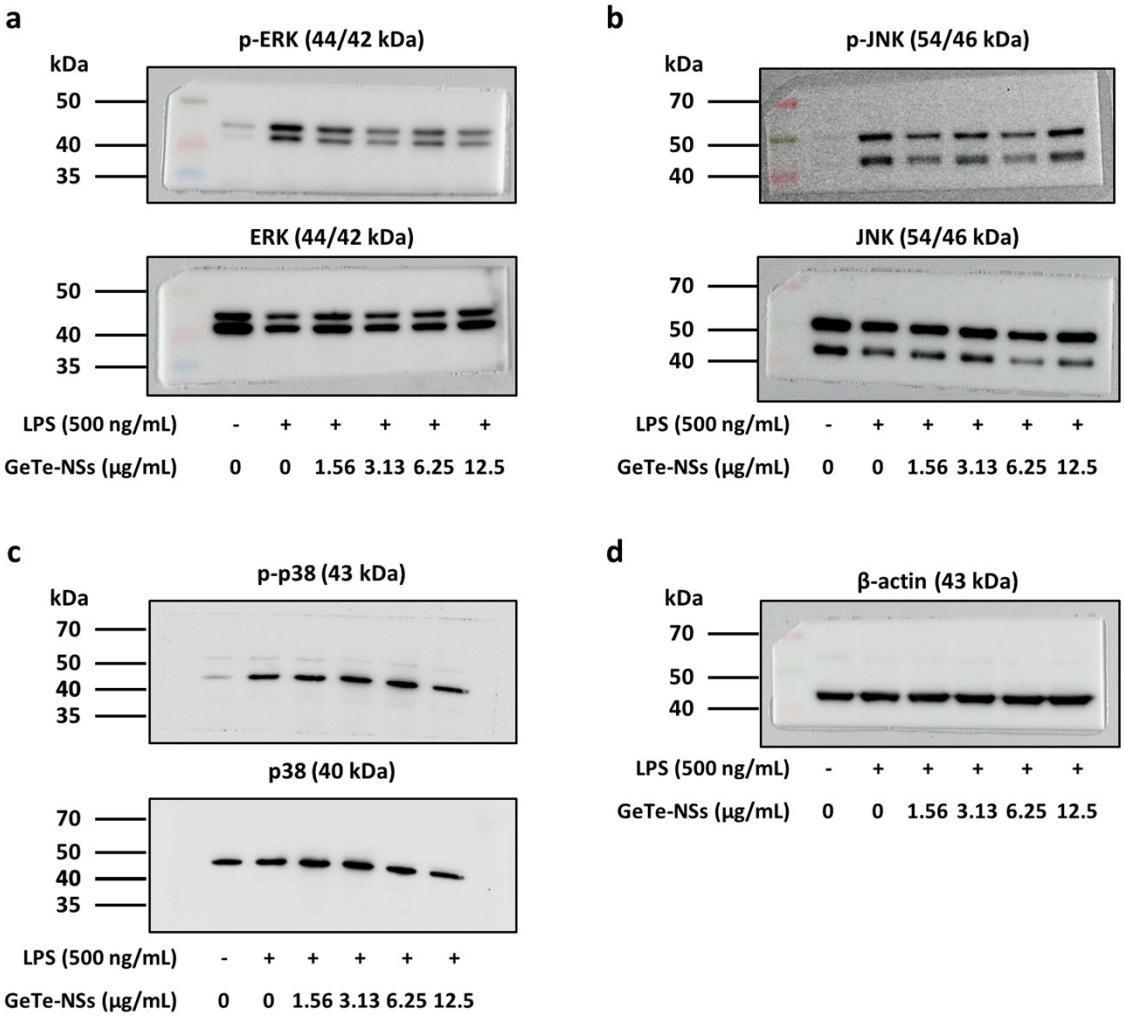

Fig. S2 Uncropped Western blot images of phosphorylated and total proteins related to MAPK pathways in RAW 264.7 cells. (a) p-ERK and ERK (stripped in order: p-ERK → ERK), (b) p-JNK and JNK (stripped in order: p-JNK → JNK), (c) p-p38 and p38 (stripped in order: p-p38 → p38). (d) β-actin. The cropped versions of these blots are shown in Fig. 5a.

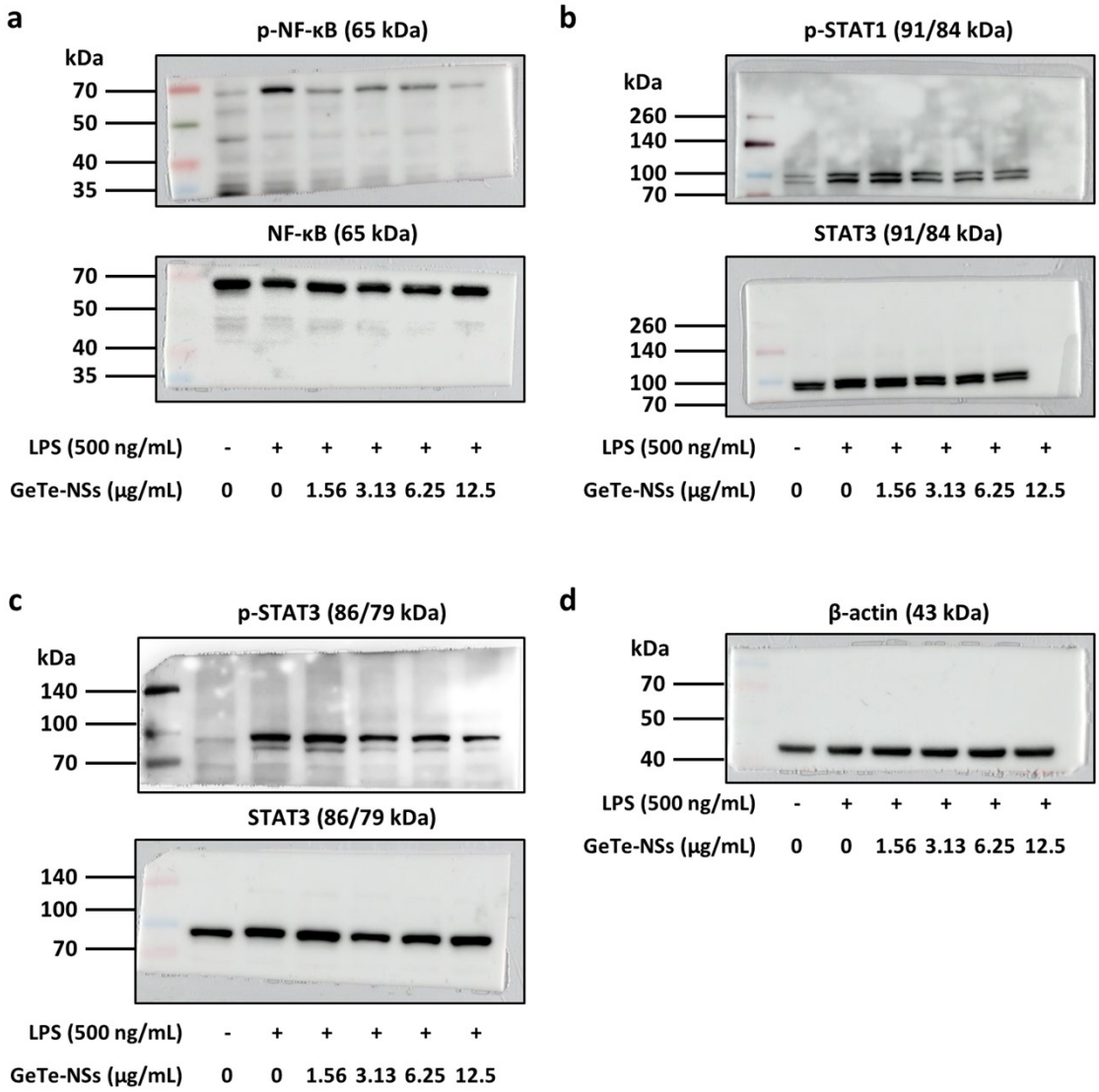

Fig. S3 Uncropped Western blot images of phosphorylated and total proteins related to NF-κB, STAT1, and STAT3 pathways in RAW 264.7 cells. (a) p-NF-κB and NF-κB (stripped in order: p-NF-κB → NF-κB). (b) p-STAT1 and STAT1 (stripped in order: p-STAT1 → STAT1). (c) p-STAT3 and STAT3 (stripped in order: p-STAT3 → STAT3). (d) β-actin. The cropped versions of these blots are shown in Fig. 5b.

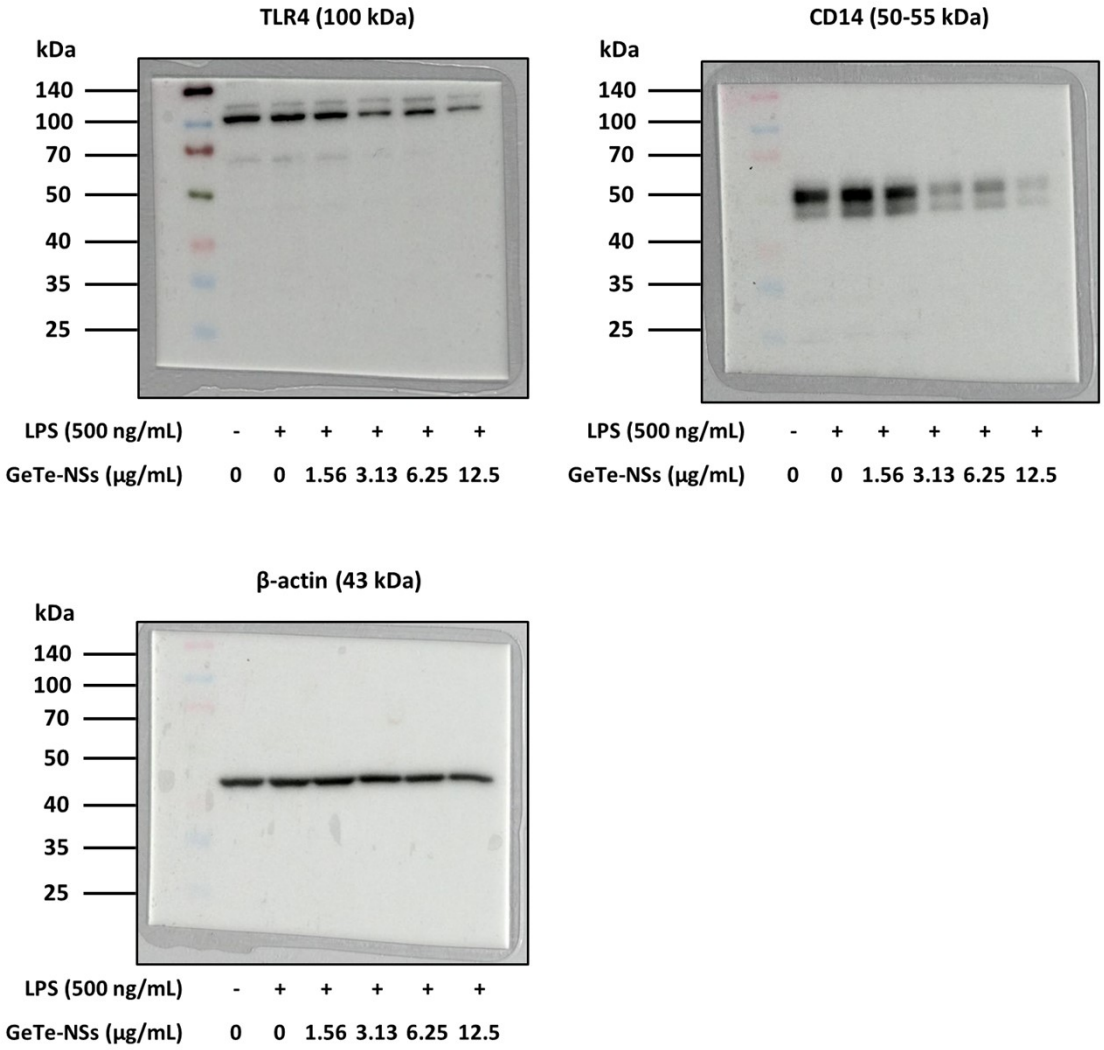

Fig. S4 Uncropped Western blot images of TLR4 and CD14 proteins in RAW 264.7 cells. TLR4, CD14, and β-actin (stripped in order: TLR4 → CD14 → β-actin). The cropped versions of these blots are shown in Fig. 5c.

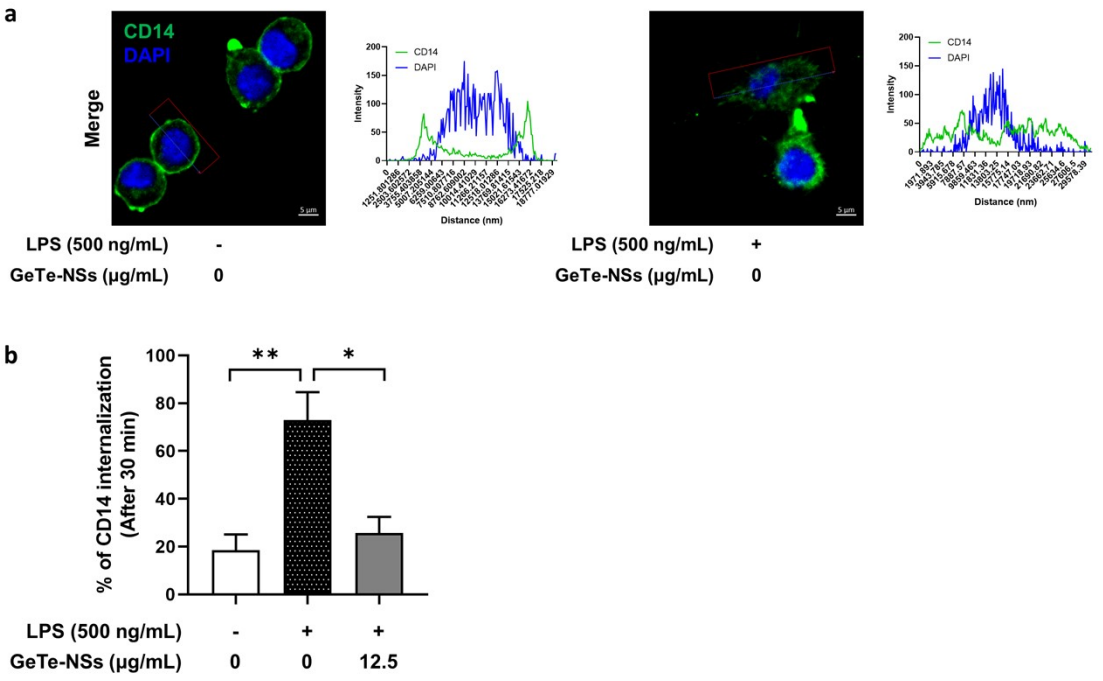

Fig. S5. After treatments as indicated for 30 min, RAW 264.7 cells were fixed and stained to assess CD14 internalization by immunofluorescence. (a) Cells on the left represent CD14-negative cells, exhibiting strong signals at the cell membrane but not in the cytoplasm, while cells on the right represent CD14-positive cells, with scattered signals in the cytoplasm. (Scale bar = 5 μm) (b) The percentage of CD14-positive cells was quantified for each group. 50–100 cells counted per samples ($n = 3$). Statistical significance was determined by one-way ANOVA in comparison with the LPS-stimulated RAW 264.7 cells. *$p < 0.05$, **$p < 0.01$.

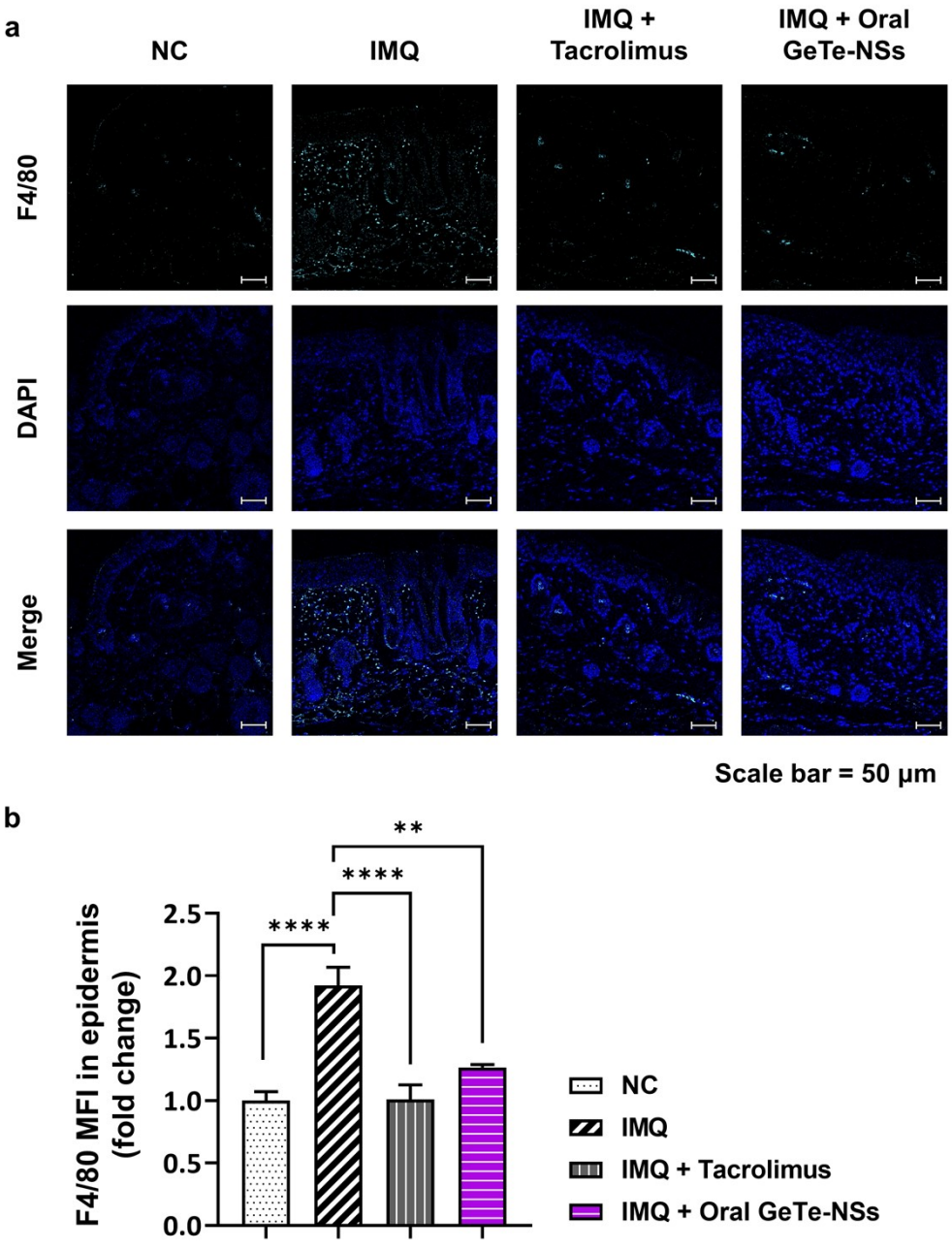

Fig. S6. Assessment of the different treatments on macrophage infiltration in the dermis. (a) Representative immunofluorescence staining images of F4/80 (light blue) and DAPI (blue) from each group (Scale bar = 50 μm). (b) Quantification of the filaggrin mean fluorescence intensity (MFI) in the epidermal lesions (n = 4). Statistical significance was determined by one-way ANOVA in comparison with the IMQ group. ns > 0.05, **p < 0.01, ****p < 0.0001.

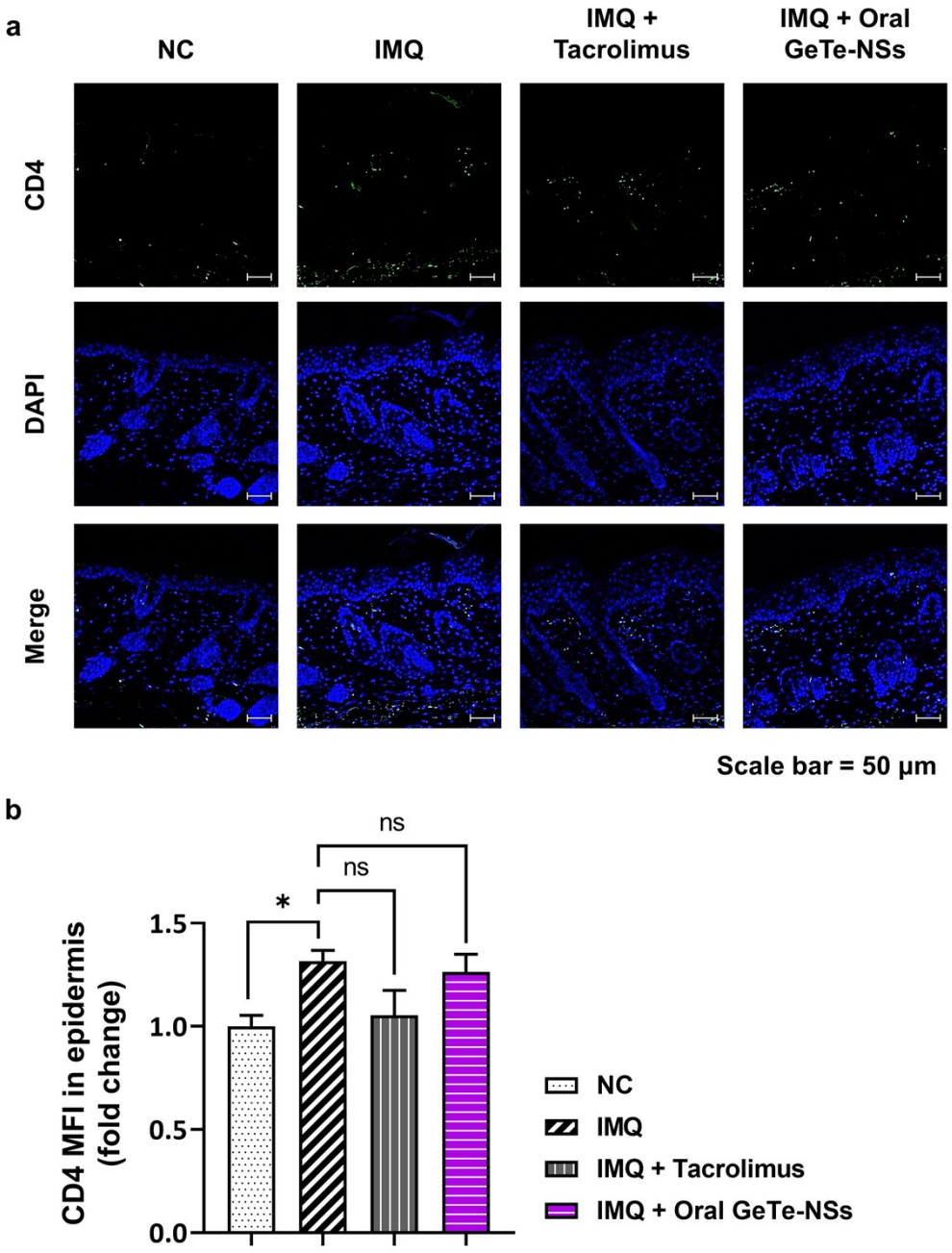

Fig. S7. Assessment of the different treatments on $CD4^+$ T cell infiltration in the dermis. (a) Representative immunofluorescence staining images of CD4 (green) and DAPI (blue) from each group (Scale bar = 50 μm). (b) Quantification of the filaggrin mean fluorescence intensity (MFI) in the epidermal lesions ($n = 4$). Statistical significance was determined by one-way ANOVA in comparison with the IMQ group. ns > 0.05, *$p < 0.05$.

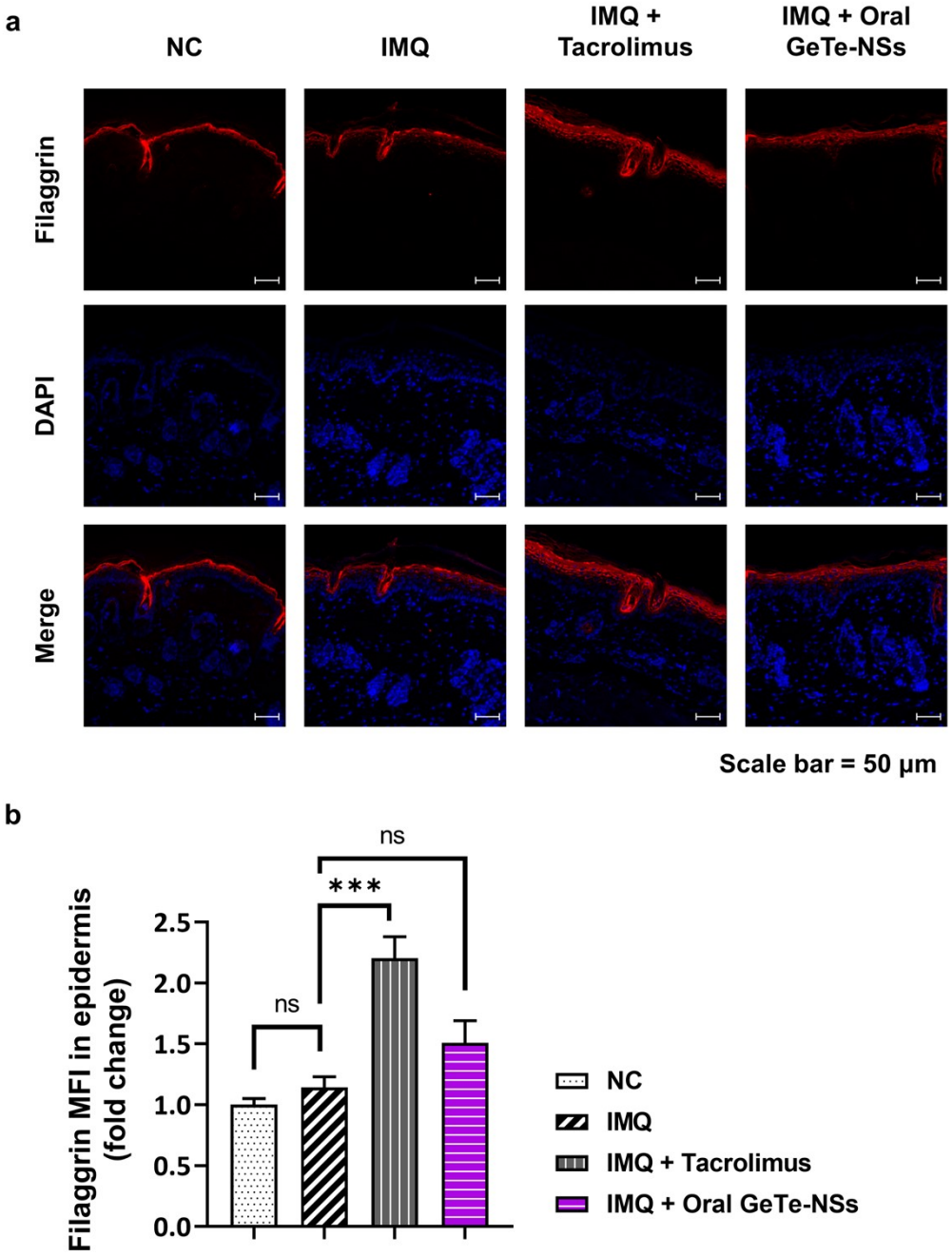

Fig. S8. Assessment of the different treatments on filaggrin expression in the epidermis. (a) Representative immunofluorescence staining images of filaggrin (red) and DAPI (blue) from each group (Scale bar = 50 μm). (b) Quantification of the filaggrin mean fluorescence intensity (MFI) in the epidermal lesions (n = 4). Statistical significance was determined by one-way ANOVA in comparison with the IMQ group. ns > 0.05, ***p < 0.001.